Retrobiosynthetic Nuclear Magnetic Resonance Analysis of Amino Acid Biosynthesis and Intermediary Metabolism. Metabolic Flux in Developing Maize Kernels[1]

Erich Glawischnig[2], Alfons Gierl, Adriana Tomas, Adelbert Bacher, and Wolfgang Eisenreich*

Lehrstuhl für Genetik (E.G., A.G.) and Lehrstuhl für Organische Chemie und Biochemie (A.B., W.E.), Technische Universität München, Lichtenbergstrasse 4, 85747 Garching, Germany; and Pioneer Hi-Bred International, 7250 NW 62nd Avenue, Johnston, Iowa 50131–0552 (A.T.)

Information on metabolic networks could provide the basis for the design of targets for metabolic engineering. To study metabolic flux in cereals, developing maize (*Zea mays*) kernels were grown in sterile culture on medium containing [U-$^{13}C_6$]glucose or [1,2-$^{13}C_2$]acetate. After growth, amino acids, lipids, and sitosterol were isolated from kernels as well as from the cobs, and their ^{13}C isotopomer compositions were determined by quantitative nuclear magnetic resonance spectroscopy. The highly specific labeling patterns were used to analyze the metabolic pathways leading to amino acids and the triterpene on a quantitative basis. The data show that serine is generated from phosphoglycerate, as well as from glycine. Lysine is formed entirely via the diaminopimelate pathway and sitosterol is synthesized entirely via the mevalonate route. The labeling data of amino acids and sitosterol were used to reconstruct the labeling patterns of key metabolic intermediates (e.g. acetyl-coenzyme A, pyruvate, phospho*enol*pyruvate, erythrose 4-phosphate, and Rib 5-phosphate) that revealed quantitative information about carbon flux in the intermediary metabolism of developing maize kernels. Exogenous acetate served as an efficient precursor of sitosterol, as well as of amino acids of the aspartate and glutamate family; in comparison, metabolites formed in the plastidic compartments showed low acetate incorporation.

The seeds of cereals are an important metabolic sink and are an essential source of human and animal nutrition. Information on the biosynthetic pathways of amino acids and vitamins in crops provides the basis for the metabolic engineering of plants with improved amino acid and vitamin profiles. In plants the pathways leading to amino acids and vitamins have been investigated in some detail at the level of enzymes and their cognate genes (for review, see Lea and Leegood, 1993; Schmid and Amrhein, 1995; Azevedo et al., 1997). Quantitative aspects of carbon flux, including transport processes under in vivo conditions have been less investigated. Incorporation of isotope-labeled precursors into plants is frequently hampered by low incorporation rates (Shimamoto and Nelson, 1981).

Isotope incorporation studies are commonly interpreted as if metabolism proceeded in a linear and unidirectional fashion. Based on this implicit assumption the diversion of isotope from a given precursor to a given target compound is accepted as evidence for direct metabolic relatedness between the respective molecular species. In reality, however, metabolism is a complex network, and metabolic flux can occur from any node in the network to virtually any other node. As a consequence, isotope incorporation studies have repeatedly resulted in remarkable errors of interpretation.

Relatively fail-safe alternatives using general ^{13}C-labeled precursors such as Glc or acetate have recently been developed for the quantitative assessment of carbon flux in bacteria and suspension cultures of plant cells (for review, see Eisenreich and Bacher, 2000). More specifically, the isotopomer composition of metabolites in biosynthetic sinks (e.g. amino acids, nucleosides, lipids, and sterols) give quantitative information about their origin. Moreover, the isotopomer pattern of central intermediates of intermediary metabolism can be reconstructed on a retrobiosynthetic basis from the data of amino acids, nucleosides, and lipids. These data reveal quantitative aspects of carbon flux and transport in the metabolic network of the organism under investigation.

In this study, we report on the incorporation of [U-$^{13}C_6$]Glc and [1,2-$^{13}C_2$]acetate into developing maize (*Zea mays*) kernels. In this culture system kernels develop under physiological conditions similar to those found in planta (Cobb and Hannah, 1983; Cully et al., 1984; Gengenbach and Jones, 1994; Glawischnig et al., 2000).

[1] This research was supported by the Deutsche Forschungsgemeinschaft (grant nos. SFB 369 and SPP 1067).

[2] Present address: Department of Plant Biology, The Royal Veterinary and Agricultural University, 40 Thorvaldsensvej, DK–1871 Frederiksberg C, Denmark.

* Corresponding author; e-mail wolfgang.eisenreich@ch.tum.de; fax 49–89–28913363.

RESULTS AND DISCUSSION

Growth Experiments with [1,2-$^{13}C_2$]Acetate

Developing maize kernels were grown in medium containing 234 mM unlabeled Suc and 36 mM [1,2-$^{13}C_2$]acetate. After 19 d of growth in the labeled medium, kernels were separated from the cob. An approximate 20 mg of sitosterol and 2 to 20 mg of amino acids were isolated from 50 g of kernels, as well as from 100 g of cob tissue.

The isolated metabolites were analyzed by ^{1}H and ^{13}C nuclear magnetic resonance (NMR) spectroscopy and absoute ^{13}C abundances were calculated by quantitative NMR spectroscopy (Table I; Eisenreich and Bacher, 2000). Figure 1 shows the ^{13}C NMR signals of Glu. The central signals marked by an asterisk represent isotopomers carrying a single ^{13}C atom that may have been formed from natural abundance Glc; alternatively, a single ^{13}C could have been contributed from labeled acetate, but only after extensive fragmentation and reassembly. The coupling satellites represent [4,5-$^{13}C_2$]- and [1,2-$^{13}C_2$]Glu at high molar concentrations, and [1,2,3-$^{13}C_3$]-, [2,3,4-$^{13}C_3$]-, and [3,4,5-$^{13}C_3$]Glu at lower concentrations. The molar fraction of each respective isotopomer in the sample was obtained from the signal integrals and normalized as described in "Materials and Methods." The isotopomer compositions of other amino acids were obtained with the same approach (Figs. 2B and 3B). The different isotopomers are all superimposed in one respective structure. The bars indicate adjacent ^{13}C atoms of each respective multiple-labeled isotopomer. The relative abundance of each isotopomer is shown by the width of the bars, as well as by the numerical subscripts.

The high ^{13}C enrichment values found in Leu and α-ketoglutarate/oxaloacetate-derived amino acids (Glu, Pro, Ile, and Asp) from cobs (Fig. 3B) suggest that the proffered acetate was efficiently incorporated into acetyl-coenzyme A (CoA) serving as precursor in the intermediary metabolism. Leu isolated from cobs was specifically characterized by 9.3% ^{13}C enrichment at C-2, and amino acids originating from the citric acid cycle intermediates, α-ketoglutarate and oxalacetate, showed ^{13}C enrichments of 5.1% to 12.1% (Table I). These high rates of ^{13}C resulted in significant ^{13}C couplings due to statistical recombination of fragments containing ^{13}C atoms. Thus, the NMR spectra of Glu and Pro showed the presence of [3,4,5-$^{13}C_3$] isotopomers at relative abundances of 19% and 20%, respectively, by statistical recombination of [$^{13}C_2$] and [$^{13}C_1$] precursors. This suggests that the citric acid cycle is driven preferentially by the proffered exogenous acetate and that endogenous synthesis of acetyl-CoA from the excess of unlabeled Suc is suppressed under these conditions. Amino acids derived from pyruvate (Val and Ala), phospho*enol*pyruvate (Tyr), and sugar phosphates (His, Tyr, and Phe) showed no significant incorporation of label (Fig. 3B; Table I). It can be concluded that in the presence of exogenous Suc, acetate or acetyl-CoA cannot be converted into the pyruvate and phospho*enol*pyruvate pool, or into the pentose phosphate cycle at significant rates.

The incorporation rates into amino acids isolated from developing kernels were lower (Table I; Fig. 2B). This suggests that the transport of acetate or acetyl-CoA from cob into kernel is reduced.

Table I. *^{13}C abundances of amino acids isolated from maize kernels or cob material labeled with [1,2-$^{13}C_2$]acetate*

n.d., Not determined.

Amino Acid	Position	Kernel	Cob
His	2	1.2	n.d.
	3	1.1	n.d.
	5	1.2	n.d.
Tyr	2	1.3	n.d.
	3	1.3	n.d.
	5/9	1.3	n.d.
	6/8	1.3	n.d.
Trp	2	1.5	n.d.
	3	1.5	n.d.
	5	1.3	n.d.
	7	1.3	n.d.
	8	1.3	n.d.
	9	1.3	n.d.
	10	1.3	n.d.
Met	2	2.9	6.1
	3	2.8	5.9
	4	1.2	1.5
Asp	2	3.9	6.0
	3	4.1	5.6
Lys	2	3.0	3.7
	3	3.3	3.2
	4	5.4	6.5
	5	3.4	3.4
	6	3.3	3.3
Glu	2	5.7	5.1
	3	5.5	7.5
	4	5.0	12.1
Val	2	1.5	1.4
	3	1.5	1.3
	4	1.5	1.2
	5	1.4	1.2
Leu	2	2.3	9.3
	3	1.5	1.7
	4	1.6	1.7
	5	1.5	1.6
	6	1.5	1.7
Ile	2	2.3	2.2
	3	1.1	1.4
	4	2.2	1.8
	5	2.4	1.9
	6	1.1	1.4
Arg	2	3.6	n.d.
	3	5.0	n.d.
	4	5.4	n.d.
	5	5.8	n.d.
Pro	2	n.d.	5.7
	3	n.d.	5.8
	4	n.d.	7.9
	5	n.d.	8.0

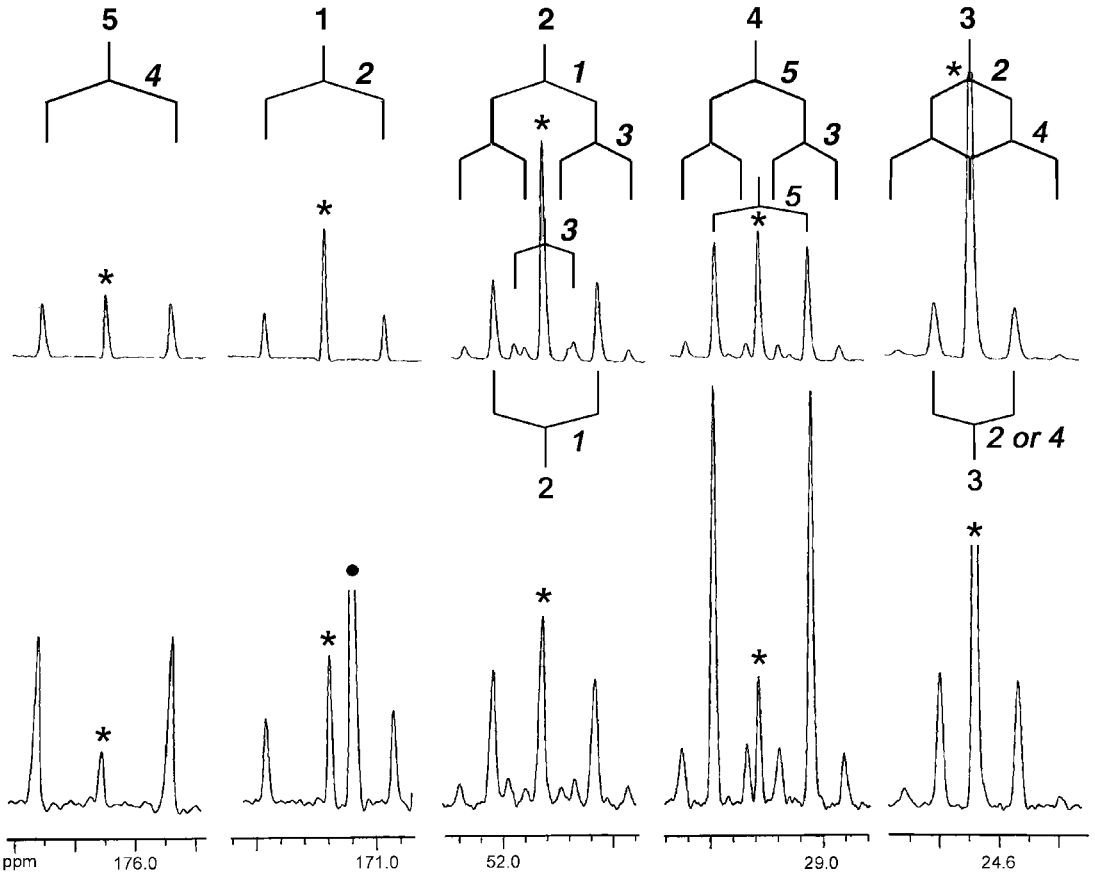

Figure 1. ^{13}C NMR spectrum of Glu isolated from kernels (top) and cob tissue (bottom) labeled with [1,2-$^{13}C_2$]acetate. Coupling patterns are indicated. Atoms ^{13}C coupled to the respective index atoms are shown in italic letters. ●, The signal of C-4 of Asp.

Growth Experiments with [U-$^{13}C_6$]Glc

Developing maize kernels were grown in medium containing 10 mM of D-[U-$^{13}C_6$]Glc (99.9% ^{13}C enrichment) and 450 mM of unlabeled D-Glc. After 19 d of growth in the labeled medium, the cell mass of kernels increased by a factor of 2.1. An approximate 20 mg of sitosterol, 20 mg of triglycerides, and 2 to 20 mg of amino acids were isolated from 50 g of kernels, as well as from 100 g of cobs.

The isolated metabolites were again analyzed by quantitative ^1H and ^{13}C NMR spectroscopy, as described above. Isotopomer compositions are summarized in Figures 2A and 3A.

The catabolism of [U-$^{13}C_6$]Glc generates multiple ^{13}C-labeled fragments that can subsequently be combined in a stochastic manner with unlabeled fragments (derived from unlabeled Glc) by anabolic reactions. Further modification of the isotope distribution pattern is possible by passage through metabolic cycles such as the pentose phosphate cycle. Every specific metabolite is therefore a mixture of different isotopomers (Figs. 2A and 3A).

Due to lower rates of de novo biosynthesis (Table II), lower relative abundances of multiple ^{13}C-labeled isotopomers were found in amino acids from cobs (Fig. 3A). However, the isotopomer compositions of amino acids isolated from cobs or kernels were qualitatively the same (Figs. 2 and 3). It can be concluded that no significant differences of metabolic flux occurred in developing kernels and their maternal tissue.

Reconstruction of Central Metabolic Intermediates and Flux Patterns by Retrobiosynthetic Analysis

The labeling pattern of central metabolites can be predicted from the isotopomer composition of amino acids based on established mechanisms (Bacher et al., 1999; Eisenreich and Bacher, 2000). More specifically, the labeling pattern of acetyl-CoA can be reconstructed from the isotopomer composition of Leu (Hagelstein and Schultz, 1993; Fig. 4).

The C1-C2 bond of acetyl-CoA is retained during glycolysis (97%). In the citric acid cycle acetyl-CoA and oxaloacetate are converted into citric acid, finally leading to α-ketoglutarate. The labeling patterns of α-ketoglutarate derived amino acids from kernels confirmed that the label of acetyl-CoA is retained in [4,5-$^{13}C_2$]ketoglutarate (100% ± 5%). However, the abundances of [1,2-$^{13}C_2$]acetyl-CoA reconstructed

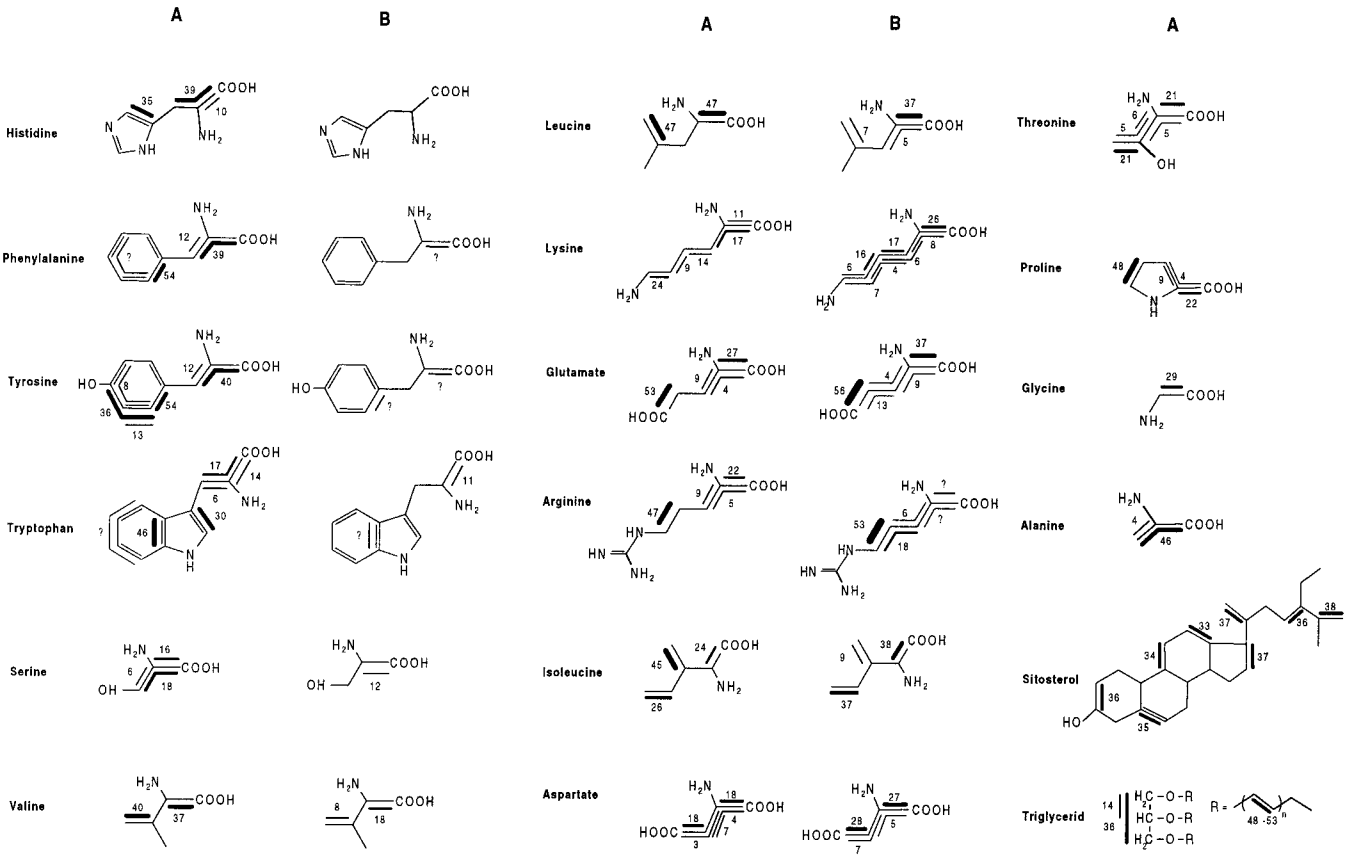

Figure 2. ^{13}C NMR data for amino acids, a triglyceride and sitosterol isolated from developing kernels labeled with [U-$^{13}C_6$]Glc (A) or [1,2-$^{13}C_2$]acetate (B). Multiple ^{13}C-labeled isotopomers are indicated as bars with a number next to the chemical bond(s) between coupled ^{13}C nuclei. The numbers represent fractions (in percentage) of multiple ^{13}C-labeled isotopomers in the overall ^{13}C-labeled isotopomer mixture of the index carbons.

from Leu (1.0 mol%) or from Arg (4.0 mol%) were significantly different (Fig. 2A; Table I). As the rates of de novo biosynthesis in the labeling period were virtually identical for Arg (44%) and Leu (42%; Table II), the different isotopomer signatures suggest two pools for acetyl-CoA. Leu biosynthesis is located in the plastids (Hagelstein and Schultz, 1993), whereas the formation of α-ketoglutarate via the citrate cycle is located in mitochondria. The lower abundance of [1,2-$^{13}C_2$]acetyl-CoA serving as precursor of Leu in the plastids indicates reduced uptake of acetate or acetyl-CoA from labeled exogenous acetate into the plastid compartment of the cell.

α-Ketoglutarate is further converted into oxaloacetate via succinate, fumarate, and malate. The labeling pattern of oxaloacetate can be gleaned from the labeling patterns of Ile and Thr (Fig. 4). Due to the symmetry of succinate and fumarate, the label from α-ketoglutarate is randomized in oxaloacetate. It is notable that significant amounts of [1,2,3-$^{13}C_3$]-, [2,3,4-$^{13}C_3$]-, and [2,3-$^{13}C_2$]-oxaloacetate were detected that cannot be explained by formation from α-ketoglutarate (Fig. 4). By comparison with the isotopomer composition of phospho*enol*pyruvate (Fig. 4), the presence of [1,2,3-$^{13}C_3$]-, [2,3,4-$^{13}C_3$]-, and [2,3-$^{13}C_2$]-oxaloacetate can be explained by partial formation of oxaloacetate (approximately 25%) via carboxylation of phospho*enol*pyruvate.

The labeling patterns of Rib 5-phosphate and erythrose 4-phosphate were reconstructed from His (Wiater et al., 1971) and the aromatic ring of Tyr (Schmid and Amrhein, 1995), respectively (Fig. 4). It is notable that we found no evidence for the presence of a [U-$^{13}C_5$]Rib isotopomer. On the other hand, the relative abundance of [U-$^{13}C_4$]erythrose phosphate was 14%. It can be concluded that the majority of the pentose phosphate intermediates are not synthesized from intact proffered [U-$^{13}C_6$]Glc, suggesting that the oxidative pentose phosphate cycle does not contribute significantly to the synthesis of Rib 5-phosphate or that futile cycling between glycolysis/pentose phosphate pathway and gluconeogenesis results in the detected cleavage and reformation of the C-3/C-4 bond of Glc-6-P.

Analysis of Lys Biosynthesis

The labeling patterns of central metabolic intermediates can be used to predict isotopomer compositions of downstream metabolites via hypothetical

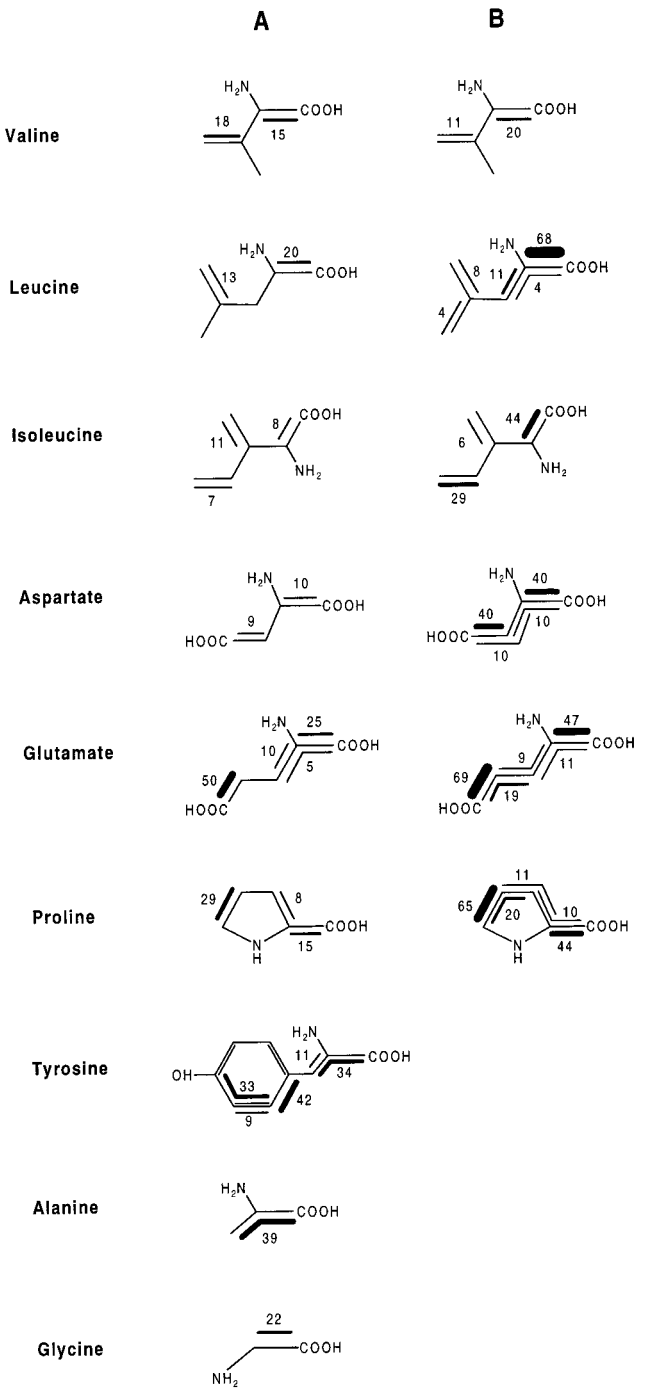

Figure 3. ^{13}C NMR data for amino acids isolated from cobs labeled with [U-$^{13}C_6$]Glc (A) or [1,2-$^{13}C_2$]acetate (B). For other details, see Figure 2.

biosynthetic pathways (Bacher et al., 1999; Eisenreich and Bacher, 2000). Figure 5 shows predictions of the labeling pattern for Lys from Asp-semialdehyde and pyruvate via meso-2,6-diaminopimelic acid and from acetyl-CoA and α-ketoglutarate. The observed labeling pattern was in almost prefect agreement with the diaminopimelate prediction. In agreement with earlier data for Lys biosynthesis in maize (Sodek, 1976), we conclude that Lys is formed exclusively via diaminopimelate and that the fungal pathway (Vogel, 1960; Jones and Broquist, 1965) via α-ketoglutarate is not operative in maize.

Analysis of Ser Biosynthesis

Ser can be synthesized from 3-phosphoglycerate or two molecules of Gly (Ho et al., 1998, 1999). As 3-phosphoglycerate can be interconverted with phospho*enol*pyruvate, identical or similar labeling patterns of phospho*enol*pyruvate and 3-phosphoglycerate can be assumed. On that basis, labeling patterns of Ser were predicted via the two alternative pathways (Fig. 6). The observed isotopomer composition of Ser indicates that both pathways contribute to its biosynthesis. From the quantitative analysis of the labeling patterns it is evident that approximately 50% of Ser are derived from phosphoglycerate and that 50% are formed from Gly (Fig. 6). These results are confirmed by the isotopomer analysis of the Trp side chain (Fig. 2A). It can be concluded that Ser biosynthesis from Gly is not restricted to photosynthetic tissue, but is also operative in non-photosynthetic developing maize kernels.

Analysis of Phytosterol Biosynthesis

It has been shown for plants and plant cell cultures that sitosterol is synthesized exclusively or predominantly via the classical mevalonic acid pathway and not via the recently discovered deoxyxylulose phosphate pathway (for review, see Eisenreich et al., 1998). Sitosterol isolated from kernels or cobs was significantly labeled from exogenous [1,2-$^{13}C_2$]acetate (>10% ^{13}C abundance), indicating that the acetyl-CoA/mevalonate pathway significantly contributes to the biosynthesis of sitosterol in maize. To quantitatively determine carbon flux leading to

Table II. *Averaged ^{13}C enrichments of amino acids isolated from maize kernels or cob material labeled with [U-$^{13}C_6$]Glc (A)*

Using these data the rates of de novo biosynthesis were calculated (B). n.d., Not determined.

Amino Acid	Kernel		Cob	
	A	B	A	B
His	2.57	59%	n.d.	n.d.
Phe	2.03	47%	n.d.	n.d.
Tyr	2.63	61%	2.13	41%
Trp	2.14	42%	n.d.	n.d.
Ser	2.30	48%	n.d.	n.d.
Val	2.08	39%	1.35	10%
Leu	2.14	42%	1.38	11%
Ile	2.34	50%	1.34	10%
Thr	2.22	45%	1.73	25%
Lys	2.12	41%	n.d.	n.d.
Arg	2.20	44%	n.d.	n.d.
Pro	2.03	37%	1.30	8%
Gly	2.30	48%	n.d.	n.d.
Ala	2.61	60%	1.60	20%

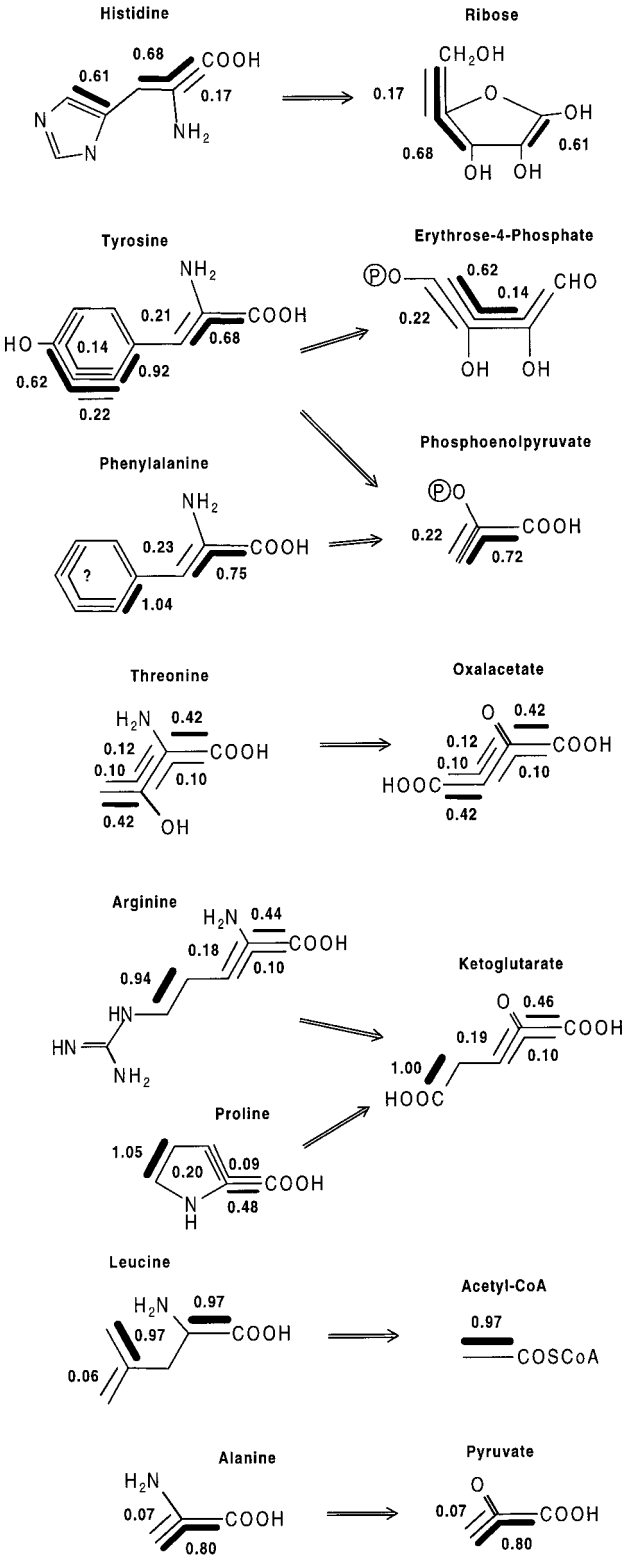

Figure 4. Reconstruction of isotopomer compositions in Rib, erythrose-4-phosphate, phospho*enol*pyruvate, oxalacetate, α-ketoglutarate, acetyl-CoA, and pyruvate by retrobiosynthetic analysis of amino acids from kernels grown in the presence of [U-$^{13}C_6$]Glc. Contiguous ^{13}C labeling is shown by bold lines. The numbers represent normalized abundances of each respective isotopomer.

sitosterol, labeling patterns of the triterpene were predicted from the labeling patterns of acetyl-CoA (as reconstructed from Leu) via mevalonate, or from glyceraldehyde 3-phosphate/phospho*enol*pyruvate (as reconstructed from Tyr) and hydroxyethyl thiamine pyrophosphate (as reconstructed from Val) via 1-deoxyxylulose 5-phosphate in the experiment with [U-$^{13}C_6$]Glc (Fig. 7). The observed labeling pattern of sitosterol perfectly matched the mevalonate prediction. Most notably, we could not observe long-range ^{13}C couplings that were predicted by a hypothetical route via 1-deoxyxylulose 5-phosphate. These results establish that sitosterol in maize kernels and cob is synthesized exclusively or predominantly (>95%) via the mevalonate pathway of terpenoid biosynthesis in agreement with studies in other plants (Schwarz, 1994; Schwender et al., 1996) and plant cell cultures (Arigoni et al., 1997).

CONCLUSIONS

The manuscript presents a new method for studying metabolic flux in developing kernels of maize. Labeling experiments with [U-$^{13}C_6$]Glc and [1,2-$^{13}C_2$]-acetate quantitatively established carbon flux of amino acid and terpenoid biosynthesis in maize kernels and cob. Moreover, it is shown that the method yields information about intermediary metabolism and transport processes over compartmental boundaries.

The method can also be used for analysis of metabolic flux under various conditions such as optimal versus stress conditions, for the comparison of different elite lines or for analysis of effects of expressing metabolic genes in transgenic plants. In the future the application of [U-$^{13}C_6$]Glc and [1,2-$^{13}C_2$]acetate could be substituted by labeling with $^{13}CO_2$ pulses. By this modification the retrobiosynthetic approach could be extended to the analysis of whole plants.

MATERIAL AND METHODS

Materials

[U-$^{13}C_6$]Glc and [1,2-$^{13}C_2$]acetate (sodium salt) were purchased from Isotec (Miamisburg, OH).

Culture of Developing Maize Kernels

Kernels were grown as described (Glawischnig et al., 2000). Four days after pollination, pieces of cob tissue each carrying four developing kernels were transferred to florist foam (Wet Foam Block, Styro-Fab, Waxahachie, TX) soaked with the culture medium containing (per liter) 80 g of unlabeled Glc (experiment with [U-$^{13}C_6$]Glc) or 80 g of unlabeled Suc (experiment with [1,2-$^{13}C_2$]acetate). Cultures were incubated at 24°C in the dark. After 7 d, kernel blocks were transferred to fresh trays with medium containing (per liter) 80 g of unlabeled Glc and 2 g of [U-$^{13}C_6$]Glc or 80 g of Suc and 3 g of [1,2-$^{13}C_2$]sodium

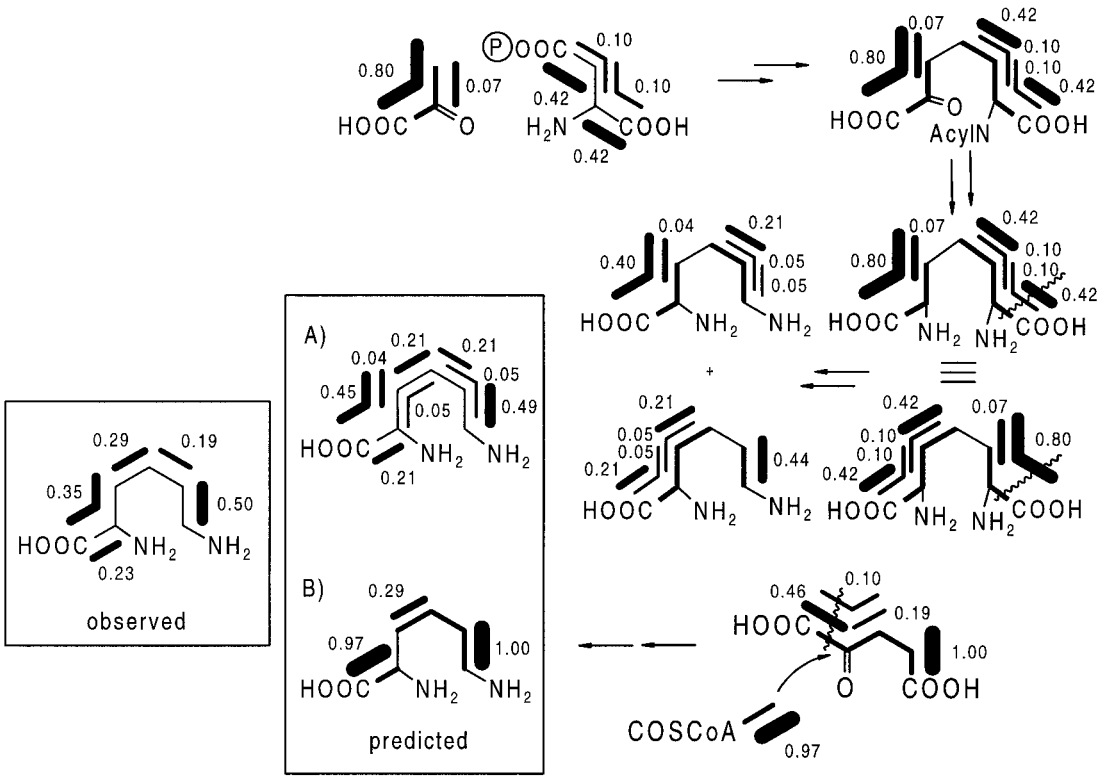

Figure 5. Comparison of observed and predicted labeling patterns of Lys from kernels grown with [U-$^{13}C_6$]Glc. These data confirm Lys biosynthesis via diaminopimelic acid (A) and exclude a significant contribution of an alternative pathway via aminoadipic acid (B). For other details, see Figure 4.

acetate, respectively. The cultures were incubated for additional 19 d, as described above.

Isolation of Metabolites

Frozen plant material (50 g of kernels or 100 g of cob pieces) were ground in liquid nitrogen, then extracted three times with 70% (v/v) acetone in water and twice with a mixture of *n*-hexane and acetone (1:1, v/v). The solvent was evaporated and the residue was dissolved in 10 mL of $CHCl_3$ and was applied on a column of silica gel 60 (40 × 6 cm), which was developed with a mixture of hexane and ethyl acetate (1:1, v/v; Arigoni et al., 1997). Fractions containing sitosterol were collected. The solvent was evaporated, and the residue was dissolved in 1 mL of $CHCl_3$. Sitosterol and triglycerides were further purified by reversed phase HPLC using a column of Lichrospher RP18 (10 × 250 mm, Merck, Rahway, NJ). The column was developed at a flow rate of 10 mL min^{-1} with methanol and the eluent was monitored photometrically (210 nm). Sitosterol and triglycerides had retention volumes of 110 and 340 mL, respectively.

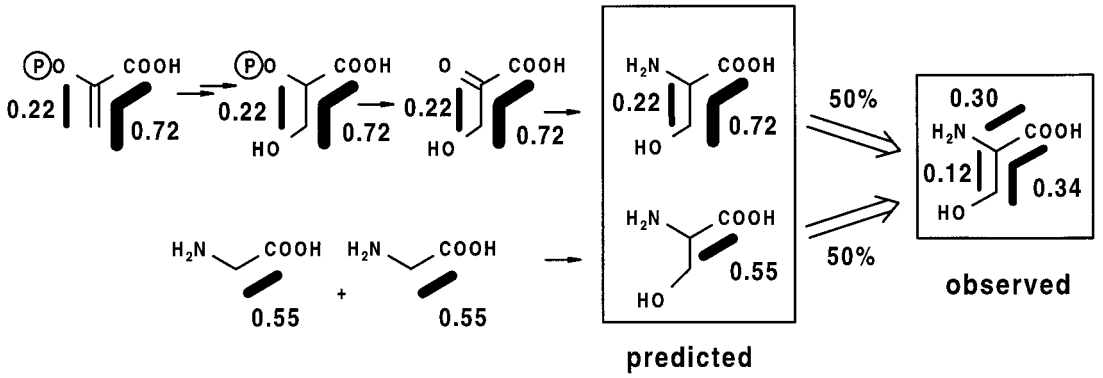

Figure 6. Comparison of observed and predicted labeling patterns of Ser from kernels grown with [U-$^{13}C_6$]Glc. The data suggest Ser biosynthesis via hydroxypyruvate, as well as from two molecules of Gly.

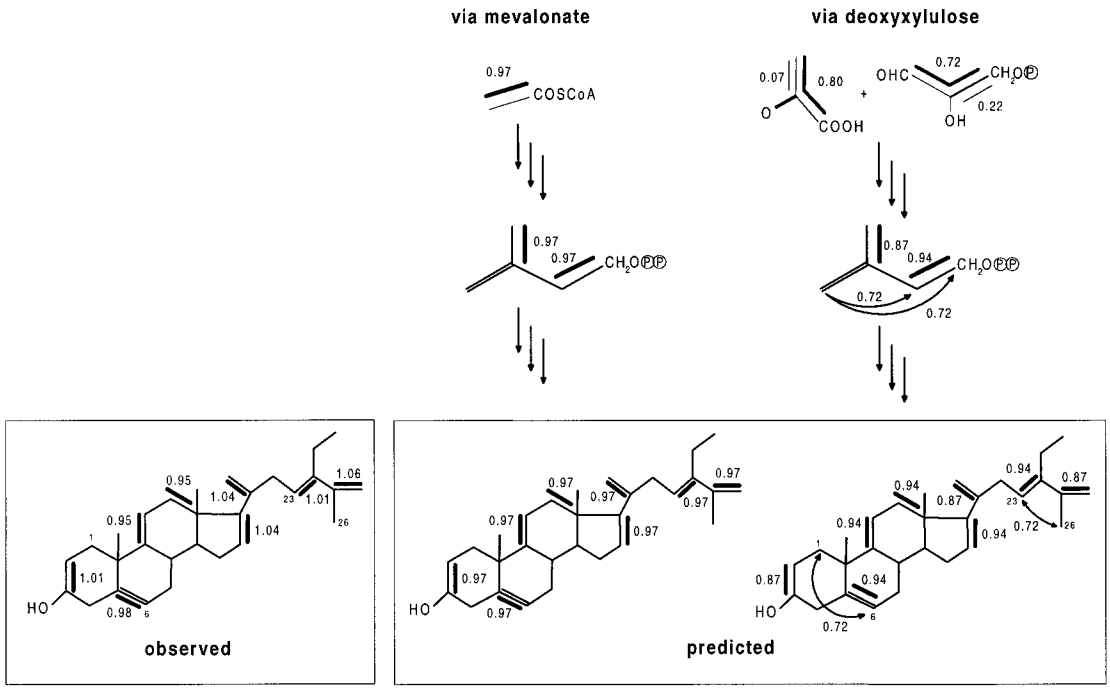

Figure 7. Comparison of observed and predicted labeling patterns of sitosterol from kernels grown with [U-$^{13}C_6$]Glc. The data demonstrate sitosterol biosynthesis via mevalonate. A hypothetical biosynthesis from 1-deoxyxylulose would result in additional long-range ^{13}C couplings, indicated by arrows, which were not observed.

A sample of the plant residue (20 g wet cell mass) was hydrolyzed at alkaline pH and Trp was isolated as described earlier (Eisenreich and Bacher, 1991). The residual plant residue (20 g wet cell mass) was heated at 110°C for 24 h in 6 M HCl containing 4% (v/v) thioglycolic acid. Amino acids were isolated from the hydrolysate as described earlier (Eisenreich et al., 1991). Val, Pro, Met, Leu, Ile, Tyr, and Phe were further purified by reversed-phase HPLC using a column of Nucleosil (21 × 250 mm, Macherey-Nagel, Düren, Germany). The column was developed at a flow rate of 10 mL min^{-1} with water. The effluent was monitored photometrically at 200 nm and 256 nm. The retention volumes were 65 mL (Pro), 75 mL (Val), 90 mL (Met), 120 mL (Leu, Ile), 150 mL (Tyr), and 310 mL (Phe). Ala, Gly, Ser, and Thr were purified by HPLC using a column of Lichrospher Si60 (10 × 250 mm, Merck). The column was eluted at a flow rate of 10 mL min^{-1} with a mixture of acetonitrile and methanol (4:1, v/v) as mobile phase. The effluent was monitored photometrically at 200 nm. The retention volumes were 26 to 44 mL (Ser and Thr) and 33 to 43 mL (Ala and Gly). Lys, His, and Arg were purified by preparative thin-layer chromatography on silica plates (Merck), which were developed with a mixture of *n*-butanol, acetic acid, and water (4:1:1, v/v). Sectors of the plate were sprayed with a solution of ninhydrine. The R_F value was 0.2 for the basic amino acids. Amino acids containing fractions were scrapped from the plates and eluted with water. The solvent was concentrated to dryness.

NMR Spectroscopy

^1H and ^{13}C NMR spectra were recorded at 500.13 and 125.76 MHz, respectively, with a spectrometer (DRX500, Bruker Instruments, Billerica, MA) as described earlier (Eisenreich and Bacher, 2000). Tyr, Trp, and Asp were dissolved in D_2O (pH 13), the other amino acids were dissolved in D_2O (pH 1). Sitosterol and triglycerides were dissolved in $CDCl_3$. ^{13}C enrichments were determined for individual positions by quantitative NMR spectroscopy (Eisenreich and Bacher, 2000). In brief, ^{13}C NMR spectra of the ^{13}C-labeled compound under study and of natural abundance material were recorded under the same experimental conditions. Integrals were determined for every ^{13}C NMR signal, and the signal integral for each respective carbon atom in the labeled compound was referenced to that of the natural abundance material, thus affording relative ^{13}C abundances for each position in the labeled molecular species.

In certain cases these relative abundances can be converted to approximate absolute enrichment by assigning a value of 1.1% to the carbon atom with the lowest ^{13}C enrichment and referencing all other carbons to that position. In other cases absolute ^{13}C enrichment can be obtained for certain atoms from ^{13}C coupling satellites in ^1H NMR spectra provided that any hydrogen atom of the compound under study is a singlet or a doublet where the coupling satellites can be determined to relatively high accuracy.

In NMR spectra of multiple-labeled samples displaying $^{13}C^{13}C$ coupling, each satellite in the ^{1}H-decoupled spectra was integrated separately. The integral of each respective satellite pair is then referenced to the total signal integrals of a given carbon atom. Normalized isotopomer compositions were calculated as described earlier (Eisenreich and Bacher, 2000; Glawischnig et al., 2000).

Received November 15, 2000; accepted December 15, 2000.

LITERATURE CITED

Arigoni D, Sagner S, Latzel C, Eisenreich W, Bacher A, Zenk MH (1997) Terpenoid biosynthesis from 1-deoxy-D-xylulose in higher plants by intramolecular skeletal rearrangement. Proc Natl Acad Sci USA **94:** 10600–10605

Azevedo RA, Arruda P, Turner WL, Lea PJ (1997) The biosynthesis and metabolism of the aspartate derived amino acids in higher plants. Phytochemistry **46:** 359–419

Bacher A, Rieder C, Eichinger D, Arigoni D, Fuchs G, Eisenreich W (1999) Elucidation of novel biosynthetic pathways and metabolite flux patterns by retrobiosynthetic analysis. FEMS Microbiol Rev **22:** 567–589

Cobb BG, Hannah LC (1983). Development of wild type, *shrunken-1* and *shrunken-2* maize kernels grown in vitro. Theor Appl Genet **65:** 47–51

Cully DE, Gengenbach BG, Smith JA, Rubenstein I, Connelly JA, Park W (1984) Endosperm protein synthesis and L-[^{35}S]methionine incorporation in maize kernels cultured in vitro. Plant Physiol **74:** 38–394

Eisenreich W, Bacher A (1991) Biosynthesis of 5-hydroxybenzimidazolylcobamide (factor III) in *Methanobacterium thermoautotrophicum*. J Biol Chem **266:** 23840–23849

Eisenreich W, Bacher A (2000) Elucidation of biosynthetic pathways by retrodictive/predictive comparison of isotopomer patterns determined by NMR spectroscopy. *In* JK Setlow, ed, Genetic Engineering, Principles and Methods, Vol 22. Kluwer Academic/Plenum Publishers, New York, pp 121–153

Eisenreich W, Schwarz M, Cartayrade A, Arigoni D, Zenk MH, Bacher A (1998) The deoxyxylulose phosphate pathway of terpenoid biosynthesis in plants and microorganisms. Chem Biol **5:** R221–R233

Eisenreich W, Schwarzkopf B, Bacher A (1991) Biosynthesis of nucleotides, flavins and deazaflavins in *Methanobacterium thermoautotrophicum*. J Biol Chem **266:** 9622–9631

Gengenbach BG, Jones RJ (1994) In vitro culture of maize kernels. *In* M Freeling, V Walbot, eds, The Maize Handbook. Springer-Verlag, Berlin, pp 705–708

Glawischnig E, Tomas A, Eisenreich W, Spiteller P, Bacher A, Gierl A (2000) Auxin biosynthesis in maize kernels. Plant Physiol **123:** 1109–1119

Hagelstein P, Schultz G (1993) Leucine synthesis in spinach chloroplasts: partial characterization of 2-isopropylmalate synthase. Biol Chem Hoppe Seyler **374:** 1105–1108

Ho CL, Noji M, Saito K (1999) Plastidic pathway of serine biosynthesis: molecular cloning and expression of 3-phosphoserine phosphatase from *Arabidopsis thaliana*. J Biol Chem **274:** 11007–11012

Ho CL, Noji M, Saito M, Yamazaki M, Saito K (1998) Molecular characterization of plastidic phosphoserine aminotransferase in serine biosynthesis from *Arabidopsis*. Plant J **16:** 443–52

Jones EE, Broquist HP (1965). Saccharopine, an intermediate of the aminoadipic acid pathway of lysine biosynthesis. J Biol Chem **240:** 2531–2536

Lea PJ, Leegood RC (1993) Plant Biochemistry and Molecular Biology. Wiley & Sons, Chichester, UK

Schmid J, Amrhein N (1995) Molecular organization of the shikimate pathway in higher plants. Phytochemistry **39:** 737–749

Schwarz MK (1994) Terpen-biosynthese in *Ginkgo biloba*: eine überraschende geschichte. PhD thesis. Eidgenössische Hochschule Zürich, Schweiz

Schwender J, Seemann M, Lichtenthaler HK, Rohmer M (1996) Biosynthesis of isoprenoids (carotenoids, sterols, prenyl side-chains of chlorophylls and plastoquinone) via a novel pyruvate/glyceraldehyde 3-phosphate non-mevalonate pathway in the green alga *Scenedesmus obliquus*. Biochem J **316:** 73–80

Shimamoto K, Nelson OE (1981) Movement of ^{14}C-compounds from maternal tissue into maize seeds grown in vitro. Plant Physiol **67:** 429–432

Sodek L (1976) Biosynthesis of lysine and other amino acids in the developing maize endosperm. Phytochemistry **15:** 1903–1906

Vogel HJ (1960) Two modes of lysine biosynthesis among lower fungi: evolutionary significance. Biochim Biophys Acta **41:** 172–173

Wiater A, Krajewska-Grynkiewicz K, Klopotowski T (1971) Histidine biosynthesis and its regulation in higher plants. Acta Biochim Pol **18:** 299–307